ELSEVIER

Journal of Photochemistry and Photobiology A: Chemistry 94 (1996) 15–26

Journal of PHOTOCHEMISTRY AND PHOTOBIOLOGY A: CHEMISTRY

Spectral properties and dynamics of the excited state structural relaxation of the ortho analogues of POPOP – Effective abnormally large Stokes shift luminophores

A.O. Doroshenko, A.V. Kirichenko, V.G. Mitina, O.A. Ponomaryov

Institute for Chemistry at Kharkov State University, 4 Svobody sqr., 310077 Kharkov, Ukraine

Received 9 November 1994; accepted 25 August 1995

Abstract

The spectral behaviour of the sterically hindered, substantially non-planar molecules of the ortho analogues of POPOP was studied by steady state absorption and fluorescence methods, time-resolved fluorescence methods and quantum chemical calculations. It was shown that the investigated molecules undergo noticeable flattening in their excited state, which leads to the essential lowering of the energy of the fluorescent term and, in turn, enlargement of the Stokes shift of the fluorescence. The flattening of the ortho analogues of POPOP in the excited state is a very effective process (estimated rate constants are of the order of 10^8–10^9 s^{-1}); it has a low activation energy and mainly intramolecular nature with a minor influence of the environment. The replacement of one of the oxazole rings in the *ortho*-POPOP molecule by an oxadiazole ring causes a near doubling of the flattening activation energy.

Keywords: Spectral properties; Dynamics; Excited state structural relaxation; Ortho analogues of POPOP

1. Introduction

The aryl derivatives of oxazole and oxadiazole are widely used as activating agents in liquid and plastic scintillators [1]. However, the small fluorescence Stokes shift values, typical of such systems, cause the significant loss of emitted light due to self-absorption and the extremely undesirable absorption of various short-lived and/or stable products of the radiation-induced decay of the plastic or liquid base of the scintillator. Thus the development of new activating agents with larger fluorescence Stokes shifts is urgent [2]. In addition, the determination of the primary photophysical or photochemical processes, which may lead to the enlargement of the Stokes shift of organic dyes in the non-polar or slightly polar media of a scintillator, is also very important. In our opinion, organic fluorophores, capable of undergoing adiabatic reversible geometry changes in their excited state, can act more effectively as activating agents in organic scintillators.

In this paper, we study the spectral properties and dynamics of the photoprocesses responsible for the abnormally large fluorescence Stokes shift values of the three ortho analogues of POPOP.

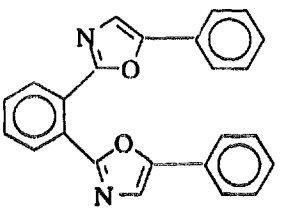

(I)

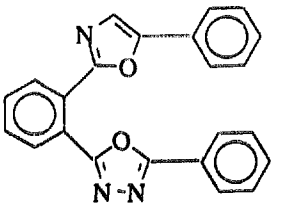

(II)

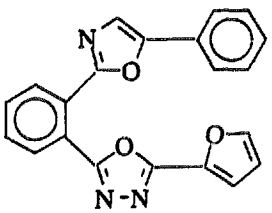

(III)

Here, **I** is 1,2-bis-(5-phenyl-oxazolyl-2)-benzene, **II** is 2-(5-phenyl-1,3,4-oxadiazolyl-2)-benzene and **III** is 2-[5-(furyl-2)-1,3,4-oxadiazolyl-2]-benzene. In previous work [3], we studied the structure of these molecules by X-ray analysis. The presence of considerable steric hindrance in the molecules of the ortho analogues of POPOP leads to the formation of significantly non-planar and non-symmetric

SSDI 1010-6030(95)04203-2

conformations. The latter are manifested by the different dihedral angles between the plane of the central phenylene ring and the planes of the oxazole/oxadiazole rings attached to it [3].

2. Experimental details

The electron absorption spectra were measured on an IBM PC AT computer-controlled Specord M40 spectrophotometer. The fluorescence spectra and quantum yields (ϕ_f) were determined on a Hitachi F4010 spectrofluorimeter. The quantum efficiency was calculated by the equation

$$\phi_x = \phi_0 \frac{S_x(1-10^{-D_0})}{S_0(1-10^{-D_x})} \quad (1)$$

where ϕ_0 is the fluorescence quantum yield of the widely used standard quinine sulphate in 1 N sulphuric acid ($\phi_0 = 0.546$ [4]), S_x and S_0 are the integrated fluorescence intensities of the corrected emission spectra of the sample and the reference solution respectively measured under the same conditions and D_x and D_0 are the corresponding optical densities at the excitation wavelengths (D values did not exceed 0.15). All spectra were measured at a temperature of 20 ± 0.1 °C. The absorption and emission spectra of compound **I** in the crystalline state were measured in thin films, obtained by the evaporation of a concentrated solution in isopropyl alcohol onto a quartz plate.

The fluorescence decay dependences and time-resolved emission spectra (TRES) were obtained on a nanosecond pulse fluorometer, containing the following main parts: (1) an air-filled, non-regulated, spark pulse lamp [5] (decay times of the pulse, depending on the adjustment of the electrodes, were in the range 1.1–1.4 ns); (2) a glass and liquid filter system (transmittance region 300–360 nm); (3) a thermostatically controlled cell holder (accuracy of the temperature ± 1 °C); (4) an MDR-12 grating monochromator; (5) a photomultiplier FEU-79; (6) a time–amplitude amplifier VAP-5 (N.N. Sevchenko Institute of Applied Physical Problems, Byelorussian University, Minsk [6]); (7) a pulse amplitude analyser AI-1024; (8) an interface to the IBM PC AT computer. The fluorescence decay data obtained were processed by the Demas and Adamson phase plane method [7], the iterative non-linear least-squares method [8,9] and by the procedure described below.

The quantum chemical calculations were carried out by the MO LCAO PPP CI (using 49 singly occupied configurations) method, upgraded by the calculation of the following special indices: electronic excitation localization numbers (L_μ) and numbers of interfragment (l_{A-B}) and intrafragment (l_{A-A}) charge transfer [10]. The calculation parameters were taken from Ref. [11]. It should be noted that the PPP method was chosen due to its high accuracy in the calculation of π–π transitions (energies and intensities in the electronic spectra of conjugated organic compounds). This method shows a more satisfactory correspondence between the calculated and experimental spectra in comparison with the spectroscopic versions of the full-valent electron semiempirical methods (CNDO, MNDO, MINDO, etc.); it is also faster and has a lower cost.

3. Time-resolved fluorescence kinetic methods

Fluorescence kinetics become complicated in the case of excited state chemical interactions and the traditional technique of treating such fluorescence decay data involves their approximation by a sum of two or more exponents. The exponent indices and pre-exponential terms exhibit a complex dependence on the kinetic constants of the primary photophysical and photochemical processes. Therefore, when it is necessary to evaluate the primary kinetic constants, the method presented below is used. [1]

Let us consider the following kinetic scheme

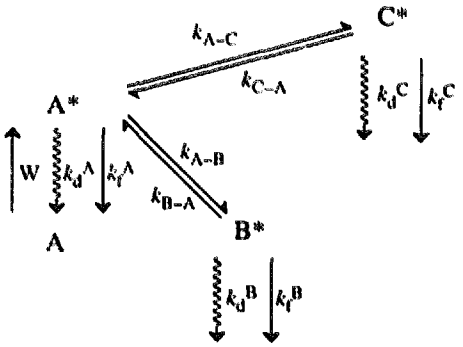

where A, B and C are the fluorescing components, the asterisks denote the excited states, W is the rate of excitation, k_f is the fluorescence rate constant, k_d is the sum of the rate constants of various radiationless processes (intersystem crossing, internal conversion $S_1^* \rightarrow S_0$, etc.) and k_{A-X} and k_{X-A} are the rate constants of the photochemical reactions $A^* \rightarrow X^*$ and $X^* \rightarrow A^*$ (they may be complex for second-order processes: $k = k'[H^+]$, $k = k'[H_2O]$, $k = k'[Q]$, etc.).

The concentration of the excited molecules A* obeys the following differential equation

$$\frac{d[A^*]}{dt} = W + \sum_{X=A,B,C...} k_{X-A}[X^*] - \left(k_f^A + k_d^A + \sum_{X=A,B,C...} k_{A-X}\right)[A^*] \quad (2)$$

[1] We call this method the multi-dimensional fluorescence phase plane method (MDFPPM), because its main calculating formula in the absence of excited state interactions is equivalent to that proposed by Demas and Adamson [7] (phase plane method). The idea of MDFPPM was proposed by Kuzmin and Sadovski [12] in 1975. Later, they used this concept for particular cases [13,14]. Our testing of MDFPPM applied to the classical system of 2-naphthol in slightly acidic media shows its applicability and satisfactory accuracy. We have re-formulated MDFPPM in Ref. [15]. We have successfully tested this method for the complex (both static and dynamic) system of 8-aminophenanthridone in aqueous sulphuric acid solutions, including up to four fluorescing components.

Let us integrate Eq. (2) within the limits from t_1 to t_2, and make the following substitutions, $[A^*]=F_A(t)/k_f^A$, $W=bE(t)$ and $\tau_A=1/(k_f^A+k_d^A+\Sigma k_{A-X})$, where $E(t)$ is the exciting pulse intensity, b is the apparatus constant, $F_A(t)$ is the integrated fluorescence of A at time t, and τ_A is the excited state A* lifetime. After dividing each term by the integral of excitation ($\int E(t)dt$), we obtain

$$\frac{F_A(t_2)-F_A(t_1)}{\int_{t_1}^{t_2}E(t)dt}=bk_f^A+\sum_{X=B,C...}k_{X-A}\frac{k_f^A}{k_f^X}\frac{\int_{t_1}^{t_2}F_X(t)dt}{\int_{t_1}^{t_2}E(t)dt}-\frac{1}{\tau_A}\frac{\int_{t_1}^{t_2}F_A(t)dt}{\int_{t_1}^{t_2}E(t)dt} \quad (3)$$

Taking into account that the total fluorescence F can be expressed as the product of the peak intensity and the area under the normalized spectral curve ($F=IS$), we obtain the final formula

$$\frac{I_A(t_2)-I_A(t_1)}{\int_{t_1}^{t_2}E(t)dt}=b\frac{k_f^A}{S_A}+$$

(Dependent variable)

$$\sum_{X=B,C...}k_{X-A}\frac{k_f^A S_A}{k_f^X S_X}\frac{\int_{t_1}^{t_2}I_X(t)dt}{\int_{t_1}^{t_2}E(t)dt}-\frac{1}{\tau_A}\frac{\int_{t_1}^{t_2}I_A(t)dt}{\int_{t_1}^{t_2}E(t)dt} \quad (4)$$

(Independent variables)

Treating the data (the corresponding ratios, using them as dependent and independent variables in the calculation scheme) for all components A–X in this static and dynamic system at every time moment between t_1 and t_2 according to Eq. (4) by the linear least-squares method (LSM), we obtain not only the lifetimes of all the excited states involved, but also the kinetic constants for all the primary photochemical processes. The calculated values of some kinetic constants may be close to zero (taking into account the error level of the approximation). This indicates the absence of photochemical interaction between the corresponding excited components. Thus the independent variables, responsible for the above-mentioned interaction, must be excluded from the LSM calculation scheme. The limits of integration (t_1 and t_2) are chosen such that the upper limit (t_2) is above the level of the apparatus noise (in our case, up to 10 counts in a channel) and the lower limit (t_1) yields the maximum value of the LSM correlation coefficient.

In the general case, the spectra of compounds A, B, ..., X are considerably overlapped. Therefore, before using Eq. (4) every peak intensity value (I_X) should be calculated by solution of the system of linear equations of the type

$$I_\lambda=\sum_{X=A,B,C...}c_X(\lambda)I_X \quad (5)$$

where I_λ is the total fluorescence intensity at wavelength λ and $c_X(\lambda)$ is the fluorescence intensity in the emission spectrum of pure compound X, normalized to the maximum. In our case, we solved the over-determined systems of linear equations of type (5) by LSM, covering all the available spectral region. Thus the method used involves the treatment of all of the fluorescence decay surface, as proposed in Refs. [16,17].

4. The nature of the electronic transitions in the absorption spectra of the ortho analogues of POPOP

The electronic absorption spectra of compounds **I–III** consist of two significantly overlapping bands in the range 25 000–45 000 cm^{-1}. The long-wavelength band appears as a shoulder on the low-frequency wing of the more intense short-wavelength band (Fig. 1, Table 1). The absorption spectra of the investigated compounds, in contrast with POPOP, are located in a shorter wavelength region and have no vibrational structure.

The results of the spectral calculation presented in Table 2 show that two different types of electronic transition are observed in the calculated absorption spectra of POPOP and **Ia** in the region 29 000–40 000 cm^{-1}: all-molecular transitions with localization mainly on the oxazolyl-phenyl fragment ($\Psi_0 \rightarrow \Psi_1$, $\Psi_0 \rightarrow \Psi_2$) and local transitions with a higher contribution on excitation of the central phenylene ring or

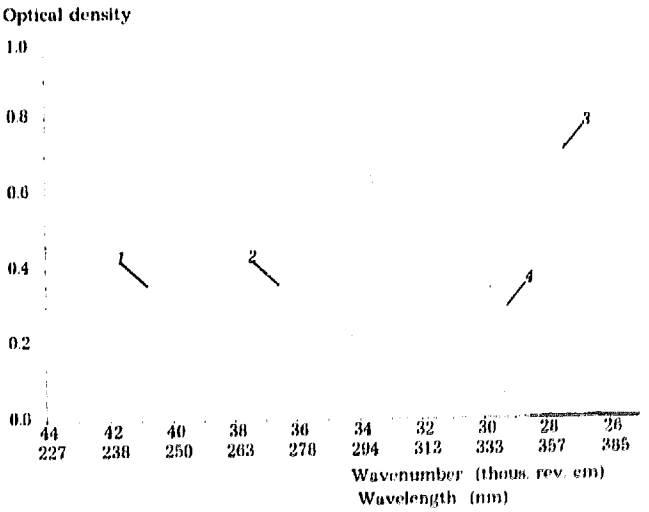

Fig. 1. Absorption spectra in octane; 1, 2-methyl-5-phenyloxazole (MPO); 2, 2,5-diphenyloxazole (PPO); 3, POPOP; 4, compound **I**.

Table 1
Spectral characteristics of the investigated and model compounds

Compound	$\nu_a^{(2)}$	$\nu_a^{(1)}$	ν_f	$\Delta\nu_{ST}$	ϕ_f
I [a]	35560	32120	23460	8660	0.550
II [a]	37200	32140	24480	7660	0.572
III [a]	36380	32140	24260	7880	0.549
MPO [a]	–	36500	31970	4530	–
PPO [a]	–	32340	28060	4280	0.607
MPD [a]	–	40600	33420	7180	–
PPD [a]	–	35260	28960	6300	–
POPOP [a]	–	27920	24420	3500	0.854
I [b]	35020	(31000)	22000	9000	–
I [c]	–	31560	23080	8480	0.492
II [c]	–	31640	23820	7820	0.454
III [c]	–	31660	23640	8020	0.463
I [d]	–	31540	22820	8720	0.558
II [d]	–	31880	22860	9020	0.576
III [d]	–	31900	22720	9180	0.570
I [e]	35900	32300	22900	9400	0.566
II [e]	37440	31920	22980	8940	0.561
III [e]	36120	32380	22900	9480	0.610
PPO [e]	–	32940	27660	5280	0.754
POPOP [e]	–	27800	23920	3880	0.796
I [f]	35640	(31640)	22680	8960	0.319
II [f]	36560	(31560)	22660	8900	0.321
III [f]	35600	(31480)	21940	9540	0.410

[a] Octane.
[b] Crystalline state.
[c] Toluene.
[d] Dimethylformamide.
[e] Isopropyl alcohol.
[f] Glycerol.
$\nu_a^{(2)}$ and $\nu_a^{(1)}$ are the absorption band maxima (cm^{-1}), ν_f is the fluorescence band maximum (cm^{-1}), $\Delta\nu_{ST}$ is the fluorescence Stokes shift (cm^{-1}) and ϕ_f is the fluorescence quantum yield. MPD, 2-methyl-5-phenyloxadiazole; PPD, 2,5-diphenyloxadiazole.

one of the terminal benzene radicals. The most significant discrepancies in the electronic excitation characteristics of POPOP and **Ia** are observed for the all-molecular transitions and the $\Psi_0 \rightarrow \Psi_3$ transition, localized mainly on the central phenylene fragment.

The single-configurational, long-wavelength, **Ia** transition $\Psi_0 \rightarrow \Psi_1$, for which the contribution of the $\phi_1 \rightarrow \phi_{1'}$ configuration is about 88%, takes place between the HOMO and LUMO, whose localization is close to the corresponding POPOP orbitals. Thus, we can conclude that the $\Psi_0 \rightarrow \Psi_1$ transitions of **Ia** and POPOP have the same nature. Significantly higher HOMO localization on the central phenylene ring in comparison with LUMO localization is responsible for the observed interfragment charge transfer with a substantial contribution from the phenylene ring, which is typical of these transitions.

The essential charge transfer between the *ortho*-phenylene fragment and the heterocyclic radicals bonded to it is also typical of the following two transitions in the **Ia** molecule, namely the all-molecular $\Psi_0 \rightarrow \Psi_2$ and mainly "benzene-type" $\Psi_0 \rightarrow \Psi_3$ α-transition (see corresponding values $l_{A\rightarrow B}$ for these transitions listed in Table 2). The charge transfer type of the mentioned transitions is caused by the significant difference in localization of the spectrally important molecular orbitals of **Ia**: high localization on the phenylene ring of the vacant $\phi_{1'}$ and $\phi_{2'}$ orbitals, and low localization on the occupied ϕ_1 and ϕ_2 orbitals in this fragment. The difference in intensity of the two long-wavelength transitions in the **Ia** and POPOP absorption spectra is caused by the more significant extension of the π-electron system of POPOP along the *X* axis and the more significant extension of the π-electron system of **Ia** along the *Y* axis.

A comparison of the experimental and calculated absorption spectra of **Ia** shows inadequate agreement (see $S_0 \rightarrow S_1$ and $S_0 \rightarrow S_2$ energies and their intensity relationship in the **Ia** spectrum, Tables 1 and 2). A set of calculations was performed, and an essential dependence of the theoretical spectrum of compound **I** on the mutual orientation of its two oxazole cycles was found. The spectrum of structure **Ib** is the closest to the experimental spectrum. However, even in this case, the correspondence between the theoretical and experimental spectra is not completely satisfactory. The non-planar conformation of the **Ib** molecule in solution is assumed to be responsible for the above-mentioned inadequate agreement. It should be noted that X-ray crystal structure analysis [3] showed essential non-planarity of molecule *I*. One oxazolyl-

Table 2
Calculated characteristics of the electronic transitions in the absorption spectra of compound I and POPOP

Transition number	ν_{max} (cm^{-1})	f	Polarization	L_{π} (%)					$l_{\mu\leftrightarrow\mu}$ (%)					$l_{\mu\leftrightarrow\nu}$ (%)
				A	B	C	D	E	A	B	C	D	E	
				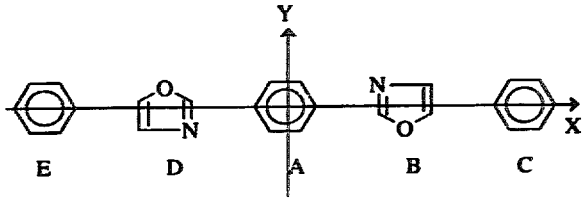										
				E D A B C										
				POPOP										
$\Psi_0 \rightarrow \Psi_1$	29600	1.84	X	32	26	8	26	8	11	11		11		$l_{A\leftrightarrow B}16$ $l_{A\leftrightarrow D}16$
$\Psi_0 \rightarrow \Psi_2$	34900	0	–	17	28	14	28	14		14	4	14	4	$l_{A\leftrightarrow B}10$ $l_{A\leftrightarrow D}10$ $l_{B\leftrightarrow C}14$ $l_{D\leftrightarrow E}14$
$\Psi_0 \rightarrow \Psi_3$	36600	0	–	74	12	1	12	1	49					$l_{A\leftrightarrow B}24$ $l_{A\leftrightarrow D}24$
$\Psi_0 \rightarrow \Psi_4$	38800	0	–	2	11	38	11	38			24		26	$l_{B\leftrightarrow C}21$ $l_{D\leftrightarrow E}23$
$\Psi_0 \rightarrow \Psi_5$	38800	0	–	2	11	38	11	38			26		24	$l_{B\leftrightarrow C}23$ $l_{D\leftrightarrow E}21$
				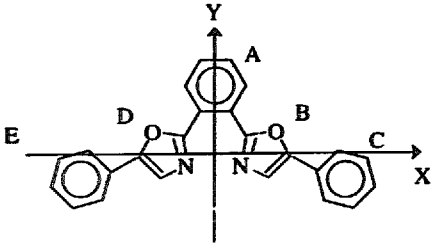										
				Ia, planar										
$\Psi_0 \rightarrow \Psi_1$	29400	1.24	X	28	28	8	28	8	8	11		11		$l_{A\leftrightarrow B}17$ $l_{A\leftrightarrow D}17$
$\Psi_0 \rightarrow \Psi_2$	33800	0.55	Y	25	26	12	26	12	8	12	4	12	4	$l_{A\leftrightarrow B}14$ $l_{A\leftrightarrow D}14$ $l_{B\leftrightarrow C}11$ $l_{D\leftrightarrow E}11$
$\Psi_0 \rightarrow \Psi_3$	34400	0.0[7]	–	59	17	3	17	3	34					$l_{A\leftrightarrow B}23$ $l_{A\leftrightarrow D}23$
$\Psi_0 \rightarrow \Psi_4$	38500	0.01		3	3	12	18	64			8		44	$l_{D\leftrightarrow E}36$
$\Psi_0 \rightarrow \Psi_5$	38600	0	–	3	18	64	3	12			43		8	$l_{D\leftrightarrow E}36$ $l_{B\leftrightarrow C}26$

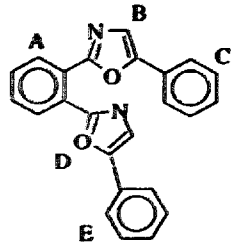

Ib, planar

$\Psi_0 \rightarrow \Psi_1$	28400	0.67	*XY*	27	31	10	26	7	8	12		10		$l_{A\leftrightarrow B}$18 $l_{A\leftrightarrow D}$14
$\Psi_0 \rightarrow \Psi_2$	33100	0.89	*XY*	32	17	6	33	13	13	5		14	4	$l_{A\leftrightarrow D}$17 $l_{A\leftrightarrow B}$13 $l_{D\leftrightarrow E}$12
$\Psi_0 \rightarrow \Psi_3$	34400	0.56	*XY*	44	26	9	16	5	23	7				$l_{A\leftrightarrow B}$21 $l_{A\leftrightarrow D}$15
$\Psi_0 \rightarrow \Psi_4$	37600	0.01	–	2	16	82					63			$l_{B\leftrightarrow C}$31
$\Psi_0 \rightarrow \Psi_5$	37700	0.01	–				16	82					64	$l_{D\leftrightarrow E}$31

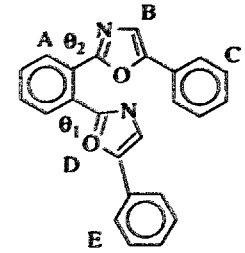

Ic, non-planar; $\theta_1 = 60°$, $\theta_2 = 30°$

$\Psi_0 \rightarrow \Psi_1$	32030	0.80	*Xy*	24	45	17	11	3	6	22	5			$l_{A\leftrightarrow B}$23 $l_{B\leftrightarrow C}$19
$\Psi_0 \rightarrow \Psi_2$	35730	1.14	*xY*	13	9	4	47	27				26	10	$l_{D\leftrightarrow E}$30
$\Psi_0 \rightarrow \Psi_3$	37050	0.04	–	59	22	5	12	2	36					$l_{A\leftrightarrow B}$28 $l_{A\leftrightarrow D}$12
$\Psi_0 \rightarrow \Psi_4$	38910	0	–	3			18	79					59	$l_{D\leftrightarrow E}$35
$\Psi_0 \rightarrow \Psi_5$	39390	0	–	5	21	74					48			$l_{B\leftrightarrow C}$41

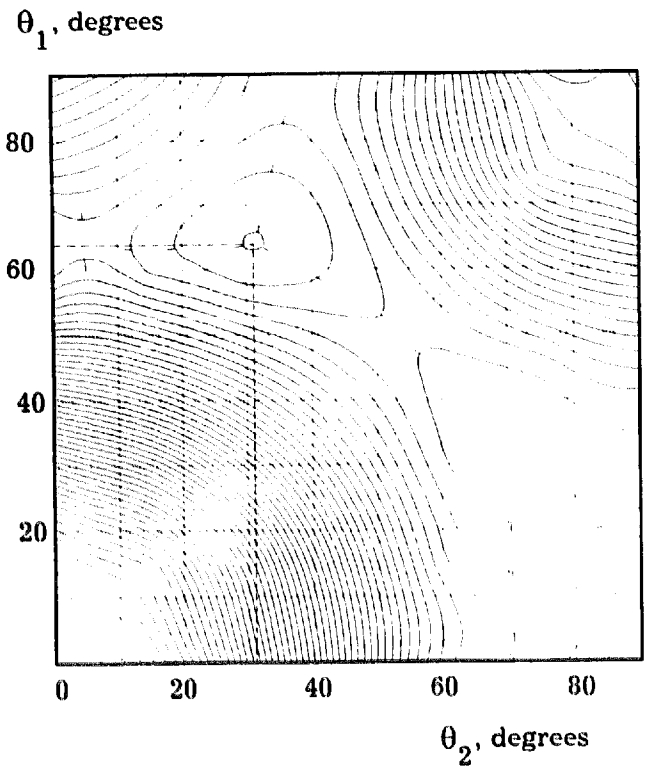

Fig. 2. Correspondence between the experimental absorption spectrum in octane and the "theoretical" absorption spectrum of compound I, calculated for torsion angles θ_1 and θ_2 in the range 0°–90° (see Table 2, structure Ic). The difference between the isolines is equal to 0.05.

phenyl fragment was rotated out of the central phenylene ring plane to an angle of approximately 67° and the other to an angle of 11°. We assume that the non-planar conformation of molecule I remains the same in solution. The absence of vibrational structure in the absorption spectrum of I (Fig. 1) also confirms this.

A set of calculations was carried out to determine the influence of non-planarity on the electronic spectrum of Ib. The rotation of the oxazole-phenyl fragments was simulated by decreasing the absolute value of the resonance integral β_{ij} of the corresponding chemical bonds proportionally to the cosine of the torsion angle ($\beta_{ij} = \beta_{ij}^0 \cos\theta$). The correlation coefficient (r) between the calculated and experimental spectra in the range 25 000–38 000 cm^{-1} was chosen as a measure of the correspondence. (To obtain the full shape of the calculated spectrum, the log-normal function [18] was used as a shape function of the individual band. The positions and intensities of the latter were taken from the quantum chemical calculation; the other parameters were as follows: bandwidth, 5000 cm^{-1}; band skewness factor, 1.2.) The most satisfactory agreement ($r \cong 0.96$, Fig. 2) between the calculated and experimental spectra was achieved for the torsion angles $\theta_1 \approx 60°$ and $\theta_2 \approx 30°$ (see Table 2). This fact and the similarity between the electronic absorption spectra in the solid state and in solution (Table 1) allow us to assume that the geometry of molecule I is approximately the same in the crystalline and dissolved states.

The calculated spectrum of molecule Ib, with one oxazolyl-phenyl fragment rotated to an angle of 60° and the other to an angle of 30° relative to the central phenylene ring, is given in Table 2. According to these results, the experimental spectrum of compound I in the range 25 000–40 000 cm^{-1} can be represented as a definite superposition of two bands of electronic transitions. The first ($\Psi_0 \rightarrow \Psi_1$) is localized on the "quasi-planar" diphenyl-oxazolyl fragment, and the second ($\Psi_0 \rightarrow \Psi_2$) is localized on the oxazolyl-phenyl fragment, rotated out of the main plane of the molecule. The long-wavelength transitions of compound I and the model 2,5-diphenyloxazole (PPO) are expected to be similar on the basis of a comparison of the corresponding excitation parameters.

The $\Psi_0 \rightarrow \Psi_2$ transition in the calculated spectrum of structure Ic is similar to the $\Psi_0 \rightarrow \Psi_1$ transition in the spectrum of the model molecule 2-methyl-5-phenyloxazole (MPO). Both transitions exhibit a large contribution from the oxazole cycle in the intrafragmental and interfragmental charge transfer ($l_{ox} = 48\%$, $l_{ox \rightarrow ph} = 29\%$).

The satisfactory correlation between the energies of graphically separated absorption bands in the experimental spectrum of compound I ($\nu_{max} = 32\,000$ and 37 000 cm^{-1}) and the corresponding model molecules PPO ($\nu_{max} = 32\,340$ cm^{-1}) and MPO ($\nu_{max} = 36\,500$ cm^{-1}) supports our assumption that the spectrum of compound I may be represented as superposition of the spectra of the model molecules.

It is interesting to note that the long-wavelength band position in the spectra of compound I–III are close to each other and also to the corresponding long-wavelength band position in the PPO spectrum. Thus we can suppose that the common structural fragment, which determines the nature of the lowest excited state of all three investigated ortho analogues of POPOP, is 2,5-diphenyl-oxazolyl. The absorption of the 5-phenyl-oxadiazolyl fragment (compound II) and the 5-furyl-oxadiazolyl fragment (compound III), rotated out of the main plane of the molecules, appears in the absorption regions of the model structures 2-methyl-5-phenyl- and 2-methyl-5-furyl-oxadiazole respectively. This determines the observed difference between the absorption spectra of compounds I–III.

Therefore, the electronic absorption spectra of the sterically hindered, substantially non-planar molecules of the ortho analogues of POPOP can be represented as a superposition of the spectra of their quasi-isolated fragments. The conjugation between the latter is considerably disrupted due to steric effects.

5. Stationary fluorescence spectra of the ortho analogues of POPOP

The fluorescence spectra of the compounds under study (Table 1, Fig. 3) are located in a longer wavelength region with respect to the emission spectra of POPOP. The fluorescence Stokes shift values exceed those typical of oxazole and

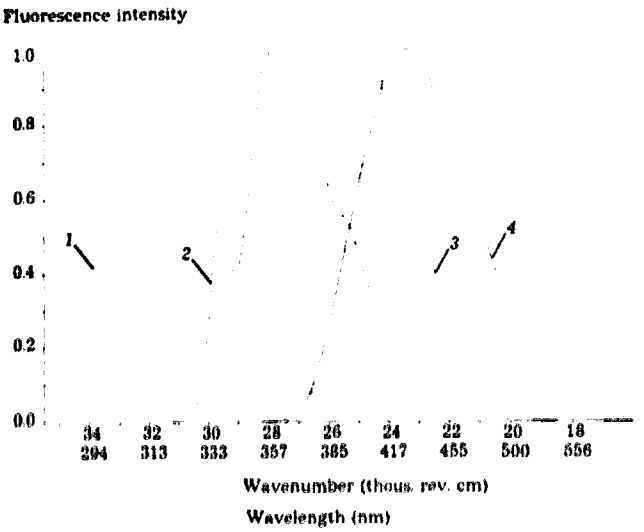

Fig. 3. Fluorescence spectra in octane: 1, 2-methyl-5-phenyloxazole (MPO); 2, 2,5-diphenyloxazole (PPO); 3, POPOP; 4, compound I.

oxadiazole aryl derivatives and vary within the range 8000–10 000 cm^{-1} depending on the nature of the solvent. The large $\Delta \nu_{ST}$ value cannot be explained only by the universal and specific interactions with the solvent: on going from non-polar octane ($\epsilon = 1.95$) to strongly polar dimethylformamide ($\epsilon = 36.7$), the magnitude of the fluorescence Stokes shift of compound I shows practically no change (Table 1). The other investigated compounds under identical conditions show $\Delta \nu_{ST}$ increases of only 1360 cm^{-1} (II) and 1300 cm^{-1} (III). The Stokes shift increase on going from octane to hydroxyl-containing solvents is of the same order. In general, the formation of H-bonded complexes with alcohol molecules is mainly exhibited as a slight broadening of the emission bands (up to 1000 cm^{-1}).

According to the results given above, we assume that the observed abnormally large fluorescence Stokes shift values are the result of the flattening of the investigated molecules in the excited state. In such a case, the conjugation between the quasi-isolated fragments of the investigated molecules is restored. This causes an essential lowering of the fluorescent state energy. It should be noted that the Stokes shift value, estimated as the difference between the calculated energy of the $\Psi_0 \rightarrow \Psi_1$ transition of molecule I with torsion angles of 10° (the full-planar structure is not probable because of steric reasons) and the ν_{max} value of the experimental fluorescence spectrum in octane, is about 5000 cm^{-1}. Such a value is typical of the series of oxazole polyaryl derivatives.

It is interesting that the flattening process of molecules I–III in the excited state also takes place in the crystalline phase. The corresponding $\Delta \nu_{ST}$ value for the crystals of compound I is high (approximately 9000 cm^{-1}).

The fluorescence quantum yields (ϕ_f) of compounds I–III are reasonably high and vary from 0.5 to 0.6 depending on the solvent. The fact that they are only slightly lower than the quantum yields of PPO and POPOP indicates that the flattening of the investigated molecules in the excited state occurs without significant radiationless loss of the excitation energy.

From the data presented in Table 1, it can be seen that the polar and proton-donating properties of the solvent have practically no influence on the ϕ_f magnitude. There is one exception to this rule: the fluorescence efficiency of I–III in glycerol is somewhat lower than in the other solvents.

6. Time-resolved fluorescence study of the ortho analogues of POPOP

Our preliminary investigations show that the fluorescence of the ortho analogues of POPOP decays more slowly than that of the commonly used para isomer. The mean fluorescence lifetimes, calculated according to the formula $\bar{\tau} = (\int t^2 I(t)dt)/(\int tI(t)dt)$, are within the range 3–5 ns depending on the experimental conditions. Therefore nanosecond pulse methods can be used to study the flattening of the ortho analogues of POPOP in the excited state. Most of our kinetic measurements were obtained in glycerol solutions to reduce the velocity of the investigated process to a maximum extent.

The excited state structural relaxation, i.e. flattening, of the studied compounds manifests itself in the essential spectral–time inhomogeneity and non-exponential nature of the fluorescence decay. The time-resolved fluorescence spectra of *ortho*-POPOP (Fig. 4) show a continuous long-wavelength shift in time (from about 23 500 cm^{-1} at 0.5 ns to approximately 22 000 cm^{-1} at 7 ns after the start of excitation of compound I in glycerol at 20 °C, Fig. 4). The initial fluorescence Stokes shift value (approximately 6000 cm^{-1}) exceeds slightly the typical value of aryl derivatives of oxazole. No time-resolved fluorescence spectra, located in the shorter wavelength region, were determined even with the

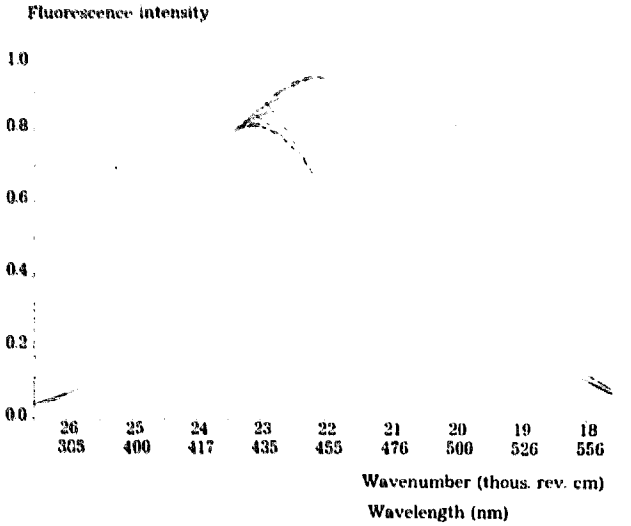

Fig. 4. Time-resolved fluorescence spectra of compound I in glycerol at 20 °C (curves approximately 1.5, 2, 2.5, 3, 4, 5, 6, 7, 8 and 9 ns after excitation; to present spectra with comparable intensity, the areas under the spectral curves were assumed to be constant).

use of a picosecond fluorometer. Therefore if the slightly enlarged Stokes shift value is due to ultrafast structural relaxation (e.g. the initial flattening of the terminal benzene rings), this may be a subject for femtosecond kinetic investigations. Here, only the slower relaxation process, relating to the nanosecond time region, is taken into account.

Phenomenologically, the treatment of structural relaxation, as well as any other kind of relaxation, may be conducted according to two different models: continuous and discrete.

In the case of the continuous relaxation model (for solvent relaxation, see the classical works by Bakhshiev et al. [19–21]; for structural relaxation in organic heterocyclic cations, see Ref. [22]), the emission occurs from each possible intermediate state, starting from the initial Franck–Condon state to the final, fully relaxed state. According to Bakhshiev, the fluorescence band shape may remain unchanged and only the shift of the emission maximum may occur.

In the case of the alternative, discrete model, the emission is observed only from the initial and final states. At any time moment after excitation, the resulting emission spectrum may be considered as a superposition of the spectra of two interacting forms. Therefore the band shape depends strongly on time: the width of the time-resolved spectrum increases up to the point at which the contributions of the two forms become equal (maximum value) and then decreases to the value typical of the final form.

It is very difficult to make a choice between the two relaxation models, because of the non-ideal apparatus time and the spectral response functions. In the present case, the width of the time-resolved fluorescence spectrum passes through a maximum at about 2.4 ns (Fig. 5). However, negative pre-exponential terms are observed in the two-exponential fluorescence decay function in the long-wavelength region, which is typical of chemical interaction in the excited state (for example, for compound I in glycerol at 20 °C and $\lambda = 500$ nm, the decay law is as follows: $0.16e^{-t/5.07} - 0.33e^{-t/0.20}$). These observations encourage us to use the discrete relaxation model for the excited state flattening of the ortho analogues of POPOP. Within the framework of the discrete relaxation model, all kinetic equations are formally similar to the corresponding equations applied to a first-order chemical reaction, and the fluorescence kinetic treatment method described above can be employed to analyse the time-resolved fluorescence data.

There are two serious circumstances that may affect the use of the MDFPP method. The first includes possible non-linear effects, e.g. reabsorption and non-stationary diffusion. In our experiments, we tried to avoid reabsorption by using dilute solutions. Non-stationary diffusion had no influence on our results, because the investigated process is first order. A second possibility involves inaccuracy in the spectral data of the pure components. The results obtained by MDFPPM (kinetic constants and lifetimes) depend strongly on the quality of the spectral separation according to Eq. (5). For the relaxation process, the spectra of both the initial and final forms are not available. We can observe only the summarized

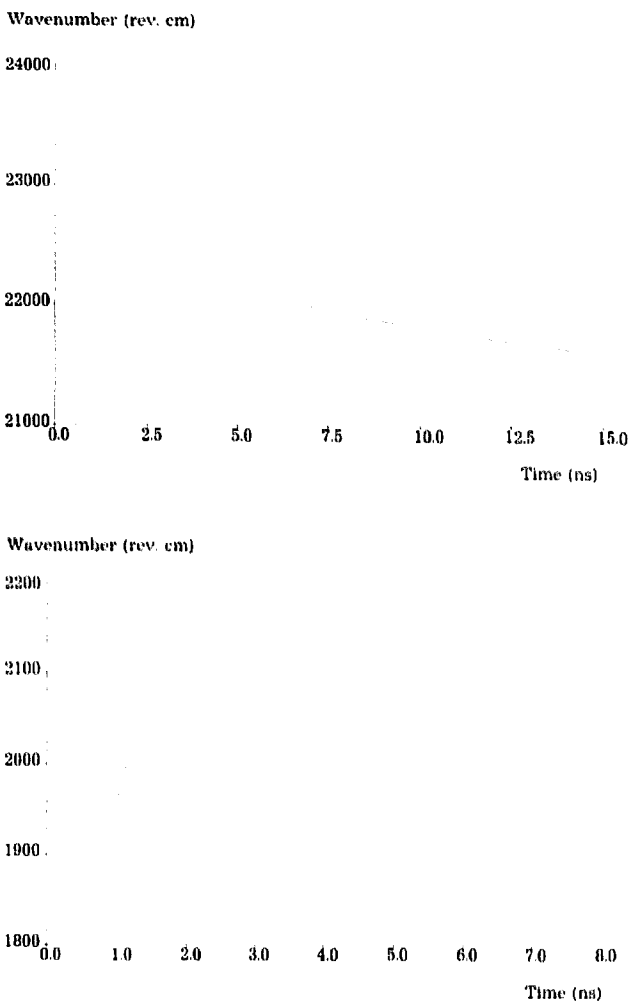

Fig. 5. The centre of mass (upper curve) and width (square root from the second central moment) of the time-resolved spectrum (lower curve) vs. time for compound I in glycerol at 20 °C.

spectrum and/or the low intensity spectrum, characterized by a poor signal-to-noise ratio (just after starting excitation, and after continuous delay when the relaxation is complete). To obtain the individual emission spectra of the interacting species, indirect methods must be used. The most satisfactory results can be obtained by the application of eigenvector analysis [23–25]. According to this method, our time-resolved fluorescence data at all experimental wavelengths (n_λ), covering the time interval from 0.4 to 12 ns (n_t), were placed into a matrix **D** of dimensions $n_t \times n_\lambda$. Then the covariance matrix $\mathbf{P} = \mathbf{D}^T\mathbf{D}$ (of dimensions $n_\lambda \times n_\lambda$, $\mathbf{D}^T$ denotes a transposed **D** matrix), its statistically valid eigenvalues $\mathbf{L}_i$ and the corresponding eigenvectors $\mathbf{V}_i$ were calculated. In all our experiments with the ortho analogues of POPOP, the number of valid eigenvalues (i.e. the rank of the covariance matrix **P**, or the number of interacting components in the system [26]) is equal to two. Obtained in such a manner, eigenvectors $\mathbf{V}_1$ and $\mathbf{V}_2$ represent the linear combination of the emission spectra of two emitting components in the sys-

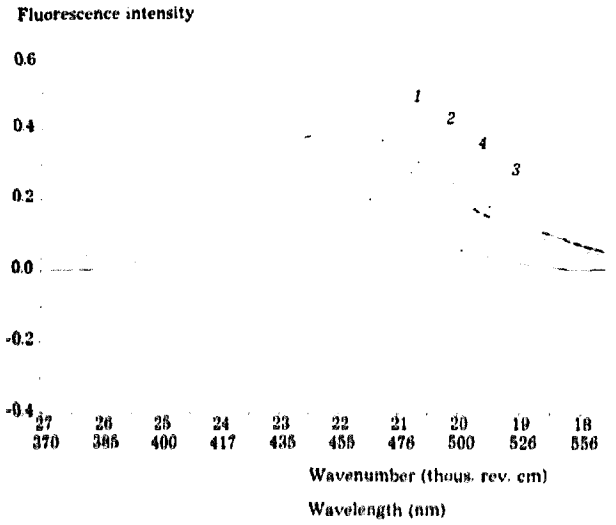

Fig. 6. Spectral separation with the use of eigenvector analysis for compound I in glycerol at 20 °C: 1, 2, two valid eigenvectors V_1 and V_2; 3, 4, individual spectra of two forms: Franck–Condon and relaxed form. Point line indicates zero intensity level.

tem studied. The individual spectra can be easily separated by a suitable selection of the $\alpha_{1,2}$ coefficients in the equation: spectrum$_{1,2} = V_1 \pm \alpha_{1,2} V_2$ (following the requirement to obtain no negative emission intensities). As an example, two calculated eigenvectors and (separated with their help) the individual spectra of the initial and final forms, involved in the relaxation process of molecule I in glycerol at 20 °C, are presented in Fig. 6.

There remains one important unresolved problem: the estimation of the value of the ratio $(k_f^0 S^0)/(k_f^1 S^1)$ (superscripts 0 and 1 denote the initial and final forms of the relaxation process). This ratio is necessary for the calculation of a true value of the relaxation rate constant. Although the k_f^0 value can be easily calculated from the experimental absorption spectrum, the value of k_f^1 cannot be obtained from any experimental data, because the excited state relaxed form does not exist in the ground state. To solve this problem, the following assumptions were made: if the Franck–Condon excited state of compound I is similar in nature to the excited state of PPO, then the k_f^0 value of compound I may be similar to the corresponding value of PPO (6.30×10^8 s^{-1}, calculated from the absorption spectrum). If, in the excited state of compound I, the conjugation between the quasi-isolated fragments of this molecule is considerably restored, then the k_f^1 value may be close to the corresponding value of a fully conjugated molecule containing the same quantity of oxazole and phenyl cycles, i.e. POPOP (6.64×10^8 s^{-1}, calculated from the absorption spectrum). Taking into account the S^0 and S^1 values (the area under the curve in the normalized fluorescence spectrum), obtained from the results of time-resolved spectral separation by eigenvector analysis, the estimation $(k_f^0 S^0)/(k_f^1 S^1) = 0.93$ was calculated for compound I.

Table 3
The results of MDFPPM treatment of the time-resolved fluorescence data of the *ortho*-POPOP analogues in glycerol at different temperatures

Compound	Temperature (°C)	τ_0 (ns)	k_- (s^{-1})	τ_1 (ns)	k_+ (s^{-1})	E_{act} (kcal mol^{-1})
I	20	1.80	–	4.42	2.69×10^8	4.92 ± 0.56
	20	1.34	–	4.61	2.80×10^8	
	20	1.51	–	4.57	2.64×10^8	
	30	1.54	–	4.74	3.72×10^8	
	40	1.56	–	4.76	4.52×10^8	
	50	1.55	–	4.72	6.96×10^8	
	60	1.28	–	4.42	7.68×10^8	
	60	1.08	–	4.41	7.58×10^8	
	60	1.31	–	4.40	7.66×10^8	
I	(Solid state)	1.88	1.75×10^8	2.14	6.03×10^7	–
II	20	2.29	–	4.37	3.78×10^8	9.6 ± 3.1
	25	1.88	4.86×10^6	3.61	6.39×10^8	
	30	1.18	2.28×10^7	4.30	7.49×10^8	
	35	1.38	1.20×10^7	3.66	13.7×10^8	
	40	0.88	8.46×10^7	3.34	12.3×10^8	
	45	0.74	4.87×10^7	2.32	19.5×10^8	
	50	0.67	1.50×10^8	1.81	22.9×10^8	
III	20	1.41	3.1×10^7	4.72	3.56×10^8	8.39 ± 0.49
	25	1.11	1.2×10^9	3.89	4.13×10^8	
	30	1.02	8.7×10^8	3.70	6.63×10^8	
	40	0.95	9.7×10^8	3.42	9.19×10^8	
	50	0.71	9.1×10^8	1.87	13.1×10^8	

τ_0 and τ_1 are the initial Franck–Condon and relaxed state lifetimes, k_+ is the flattening kinetic rate constant, k_- is the kinetic rate constant for the reverse process and E_{act} is the Arrhenius activation energy of flattening.

Although our assumptions are rather approximate, the values of such ratios are almost unity within experimental error for all investigated compounds.

The analysis of the time-resolved fluorescence data by MDFPPM is presented in Table 3. The data obtained show a high efficiency of the investigated photoprocess; the corresponding rate constants are of the order of 10^8–10^9 s^{-1}. It is interesting to note that the flattening of the *ortho*-POPOP analogues is practically irreversible in solution. A different behaviour is observed in the crystalline state. In this case, changes typical of the studied relaxation process are also revealed in the time-resolved fluorescence spectrum. However, in contrast with solutions, the unflattening is approximately doubly effective in the solid state.

We have also investigated the influence of temperature on the structural relaxation of the ortho analogues of POPOP to estimate the height of the potential barrier between the Franck–Condon and relaxed states. (Our Moscow colleagues have reported the barrierless structural relaxation of some organic heterocyclic cations [22]. For the other case of structural relaxation, the well-studied formation of twisted intramolecular charge transfer (TICT) states, a noticeable potential barrier was found [27].) The temperature investigation carried out for glycerol solutions was also aimed at determining the influence of viscosity on the studied process. The corresponding Arrhenius activation energies are presented in Table 3. It can be seen that, for compounds I–III, the flattening activation energies are considerably lower than the viscosity activation energy of glycerol (17.6 kcal mol^{-1}). This demonstrates that the medium viscosity does not have a determining effect on the investigated structural relaxation. An analogous conclusion can be made with respect to the polarity and proton-donating ability of the solvent by analysis of the steady state fluorescence data (Table 1). Therefore the excited state flattening of *ortho*-POPOP analogues is mainly an intramolecular process, and the influence of the environment is of minor importance.

It is interesting that the replacement of one of the oxazole rings in compound I by an oxadiazole ring causes a near doubling of the flattening activation energy. Further changes in structure (cf. compounds II and III) have practically no effect on the height of the potential barrier of the relaxation. Therefore only structural changes in the neighbourhood of the chemical bond, around which intramolecular rotation occurs, have an influence on the investigated process.

7. Conclusions

The spectral and luminescence properties of the sterically hindered, substantially non-planar, asymmetric molecules of the ortho analogues of POPOP were studied. It was found that, due to non-planarity, the conjugation between the diphenyl-oxazolyl and oxazolyl(oxadiazolyl) aryl fragments of the molecules is noticeably disrupted, and the electronic absorption spectra of the investigated compounds can be represented as a superposition of the spectra of the quasi-isolated fragments

It was shown that the molecules of the ortho analogues of POPOP undergo noticeable flattening in their excited singlet state. This process occurs without significant radiationless loss of excitation energy. The excited state flattening causes an essential lowering of the energy of the fluorescent state and is responsible for the observed abnormally large Stokes shift values.

The excited state flattening of the ortho analogues of POPOP is a very effective process, which has a low activation energy and is mainly of intermolecular nature with a minor influence of the environment. Only structural changes in the neighbourhood of the chemical bond, around which intramolecular rotation occurs, influence the magnitude of the flattening activation energy.

Acknowledgements

This work was supported in part by the George Soros' International Science Foundation (grant U37000) and the Ukrainian Fund of Fundamental Research (project 3.3/62). We are grateful to L.D. Patsenker (Ukrainian Academy of Science, Institute for Single Crystals, Kharkov) for provision of compounds I–III. Thanks are also due to Yu.V. Maliukin and N.L. Pogrebniak (Ukrainian Academy of Sciences, Institute for Single Crystals, Kharkov) for conducting the preliminary picosecond investigations.

References

[1] J.B. Birks, *The Theory and Practice of Scintillation Counting*, Pergamon, Oxford, 1967.
[2] C. Zorn, M. Bowen, S. Majewski, J. Walker, R. Wojcik, C. Hurlbut and W. Moser, *Nucl. Instrum. Methods Phys. Res. A, 273* (1988) 108.
[3] A.O. Doroshenko, L.D. Patsenker, V.N. Baumer, L.V. Chepeleva, A.V. Van'kevich, A.V. Kirichenko, S.N. Yarmolenko, V.M. Scherschukov, V.G. Mitina and O.A. Ponomaryov, *Mol. Eng., 3* (1994) 353.
[4] W.H. Melhuish, *J. Phys. Chem., 65* (1961) 229.
[5] F.A. Ermalitsky and I.E. Zalesski, *Zh. Prikl. Spektrosk., 38* (1983) 550.
[6] E.S. Voropai, S.M. Dmitriev and F.A. Ermalitsky, *Prib. Tekh. Eksp.*, (1986) 241.
[7] J.N. Demas and A.W. Adamson, *J. Phys. Chem., 75* (1971) 2463.
[8] W.R. Ware, L.J. Doemeny and T.L. Nemzek, *J. Phys Chem., 77* (1973) 2038.
[9] A. Grinvald and I.Z. Steinberg, *Anal. Biochem., 59* (1974) 583.
[10] A.V. Luzanov, *Usp. Khim., 69* (1980) 2086.
[11] J. Griffits, *Dyes Pigments, 3* (1982) 211.
[12] M.G. Kuzmin and N.A. Sadovski, *Khim. Vys. Energ., 9* (1975) 291.
[13] A.B. Demjaschkewitch, N.K. Zaitsev and M.G. Kuzmin, *Dokl. Akad. Nauk SSSR, 231* (1976) 126.
[14] A.B. Demjaschkewitch, N.K. Zaitsev and M.G. Kuzmin, *Chem. Phys. Lett., 55* (1978) 80.
[15] O.A. Ponomaryov, A.O. Doroshenko and V.G. Mitina, *Khim. Fiz., 8* (1989) 1369.
[16] J.M. Beechem, M. Amelot and L. Brand, *Chem. Phys. Lett., 120* (1985) 466.

[17] M. Amelot, J.M. Beechem and L. Brand, *Chem. Phys. Lett., 129* (1986) 211.
[18] D.B. Siano and D.E. Metzler, *J. Chem. Phys., 51* (1969) 1856.
[19] N.G. Bakhshiev, Yu.T. Mazurenko and I.V. Piterskaya. *Opt. Spektrosk., 21* (1966) 550.
[20] N.G. Bakhshiev, Yu.T. Mazurenko and I.V. Piterskaya, *Izv. Akad. Nauk SSSR, Ser. Fiz., 32* (1968) 1360.
[21] Yu.T. Mazurenko and N.G. Bakhshiev, *Opt. Spektrosk., 28* (1970) 905.
[22] B.M. Uzhinov, S.L. Dmitruk and S.I. Druzhinin, *XVI Int. Conf. on Photochemistry, Vancouver, 1993*, p. 419.
[23] J.L. Simonds, *Opt. Soc. Am., 53* (1963) 968.
[24] I.M. Warner, G.D. Christian, E.R. Davidson and J.B. Callis, *Anal. Chem., 49* (1977) 564.
[25] H. Gampp, M. Haeder, C.J. Meyer and A.D. Zuberbuhler, *Talanta, 33* (1986) 943.
[26] D. Katakis, *Anal. Chem., 37* (1965) 876.
[27] Z.R. Grabovski, *Acta Phys. Polon., A71* (1987) 743.